遺伝専門医制度<http://jshg.org>と，認定遺伝カウンセラー制度<http://plaza.umin.ac.jp/~GC/>により，遺伝カウンセリングを担当する人材養成が行なわれている。臨床遺伝専門医は日本人類遺伝学会と日本遺伝カウンセリング学会が認定している専門医資格であり，基本領域の専門医を取得した後，3年間の研修を経て，専門医認定試験の受験資格を得ることができる。2010年9月現在，603名が認定されている。一方，非医師を対象とした認定遺伝カウンセラーは，日本人類遺伝学会と日本遺伝カウンセリング学会が認定しているもので，現在9大学の修士課程にその養成コースが設けられており，2010年9月現在，74名が認定されている。

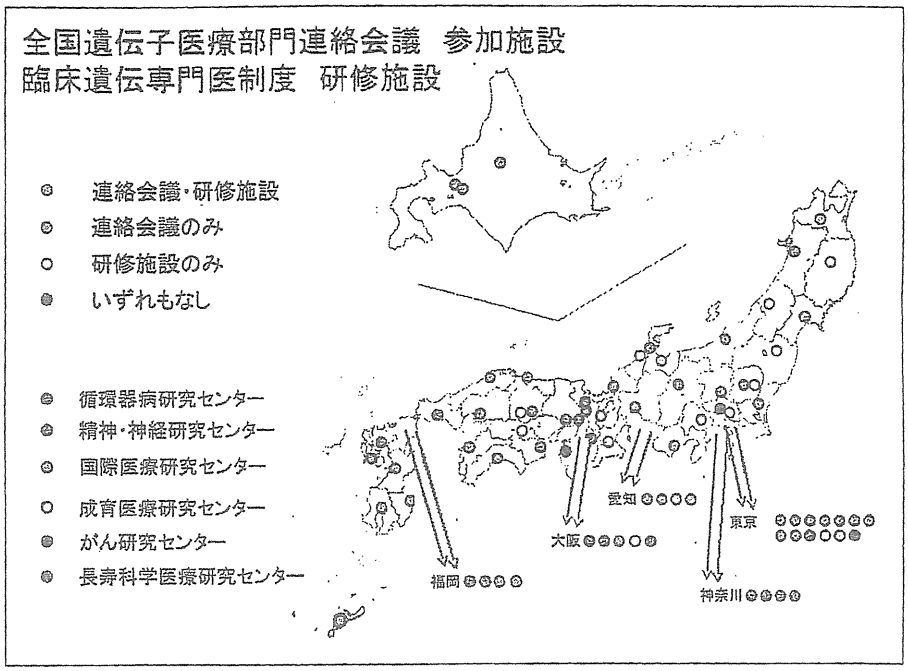

図2　全国遺伝子医療部門連絡会議に加盟している大学病院および国立高度医療機関

6. 全国遺伝子医療部門連絡会議との連携

ヒトゲノム解析研究の進展とともに，あらゆる医療の領域において，種々の遺伝学的検査法が開発されている。遺伝学的検査により明らかにされる遺伝情報は生涯変化せず，将来を予測し得る情報であり，他の血縁者にも影響を与え得るものであり，遺伝学的検査を実施する医療施設，特に大学病院をはじめとする高度医療機関においては，適切な遺伝カウンセリングの実施体制を整えるなど，遺伝子医療の充実が求められている。

全国遺伝子医療部門連絡会議は，遺伝子医療部門の存在する高度医療機関（大学病院，臨床遺伝専門医研修施設，等）の代表者により構成され，わが国の遺伝子医療（遺伝学的検査および遺伝カウンセリング，等）の充実・発展のための活動を行っている。

平成22年度現在，89の医療機関（75の大学病院と14のその他の病院・教育機関）が加盟し，遺伝子医療が抱える種々の問題解決のための活動を行い，その成果を報告書，および本ホームページ上で公表している<http://www.idenshiiryoubumon.org/>（図2）。

倫理的問題に対応する必要がある場合や，当事者がまだ発症していないような場合には，全国各地に設立されている遺伝子医療部門と連携をとることが望まれる。

おわりに

以上，臨床遺伝医療について，私見を交えて解説した。各診療科の診療に種々の遺伝学的検査と遺伝カウンセリングを欠かすことはできない。必要に応じて，各地に設置されつつある遺伝子医療部門と連携をとり，よりレベルの高い臨床遺伝医療が実現されることを願いたい。

RESEARCH ARTICLE

AMERICAN JOURNAL OF
medical genetics
Neuropsychiatric Genetics

A Loss-of-Function Mutation in the *SLC9A6* Gene Causes X-Linked Mental Retardation Resembling Angelman Syndrome

Yumi Takahashi,[1] Kana Hosoki,[1] Masafumi Matsushita,[2] Makoto Funatsuka,[3] Kayoko Saito,[4] Hiroshi Kanazawa,[2] Yu-ichi Goto,[5] and Shinji Saitoh[1]*

[1]Department of Pediatrics, Hokkaido University Graduate School of Medicine, Sapporo, Japan

[2]Deparrtment of Biological Sciences, Graduate School of Science, Osaka University, Osaka, Japan

[3]Department of Pediatrics, Tokyo Womens' Medical University, Tokyo, Japan

[4]Institute of Medical Genetics, Tokyo Womens' Medical University, Tokyo, Japan

[5]Department of Mental Retardation and Birth Defect Research, National Institute of Neuroscience, National Center of Neurology and Psychiatry, Tokyo, Japan

Received 29 November 2010; Accepted 6 July 2011

SLC9A6 mutations have been reported in families in whom X-linked mental retardation (XMR) mimics Angelman syndrome (AS). However, the relative importance of *SLC9A6* mutations in patients with an AS-like phenotype or XMR has not been fully investigated. Here, the involvement of *SLC9A6* mutations in 22 males initially suspected to have AS but found on genetic testing not to have AS (AS-like cohort), and 104 male patients with XMR (XMR cohort), was investigated. A novel *SLC9A6* mutation (c.441delG, p.S147fs) was identified in one patient in the AS-like cohort, but no mutation was identified in XMR cohort, suggesting mutations in *SLC9A6* are not a major cause of the AS-like phenotype or XMR. The patient with the *SLC9A6* mutation showed the typical AS phenotype, further demonstrating the similarity between patients with AS and those with *SLC9A6* mutations. To clarify the effect of the *SLC9A6* mutation, we performed RT-PCR and Western blot analysis on lymphoblastoid cells from the patient. Expression of the mutated transcript was significantly reduced, but was restored by cycloheximide treatment, indicating the presence of nonsense mediated mRNA decay. Western blot analysis demonstrated absence of the normal NHE6 protein encoded for by *SLC9A6*. Taken together, these findings indicate a loss-of-function mutation in *SLC9A6* caused the phenotype in our patient.** ©2011 Wiley-Liss, Inc.

Key words: *SLC9A6*; sodium/hydrogen exchanger 6; Angelman syndrome; X-linked mental retardation; nonsense mediated mRNA decay

How to Cite this Article:
Takahashi Y, Hosoki K, Matsushita M, Funatsuka M, Saito K, Kanazawa H, Goto Y-I, Saitoh S. 2011. A Loss-of-Function Mutation in the *SLC9A6* Gene Causes X-Linked Mental Retardation Resembling Angelman Syndrome.
Am J Med Genet Part B 156:799–807.

INTRODUCTION

SLC9A6 mutations were first reported by Gilfillan et al. [2008] in families exhibiting an X-linked mental retardation (XMR) syndrome mimicking Angelman syndrome (AS). Angelman syndrome is characterized by severe developmental delay with absent or minimal speech, ataxia, easily provoked laughter, epilepsy, and microcephaly. The syndrome is caused by loss-of-function of the *UBE3A* gene which is subject to genomic imprinting. Patients with *SLC9A6* mutations resemble patients with AS, but also demonstrate distinctive clinical features including cerebellar atrophy, slow progression of symptoms, increased glutamate/glutamic acid peak on magnetic resonance spectroscopy (MRS), and lack of characteristic abnormalities seen AS patients examined using electroencephalography (EEG). Following the first report in 2008, in 2010 Schroer et al. reported two other families with AS due to *SLC9A6* mutations, and confirmed the findings of Gilfillan et al.

The *SLC9A6* gene is located on Xq26.3, and encodes the ubiquitously expressed Na^+/H^+ exchanger protein member 6, NHE6. The NHE protein family consists of nine members and includes

Grant sponsor: Ministry of Education, Culture, Sports, Science, and Technology, Japan; Grant number: 21591306.
*Correspondence to:
Shinji Saitoh, Department of Pediatrics, Hokkaido University Graduate School of Medicine, N-15, W-7, Kita-ku, Sapporo 060-8638, Japan.
E-mail: ss11@med.hokudai.ac.jp
Published online 2 August 2011 in Wiley Online Library (wileyonlinelibrary.com).
DOI 10.1002/ajmg.b.31221

NHE1-5 which is found in the plasma membrane, and NHE6-9 which is found in the membranes of intracellular organelles such as mitochondria and endosomes. NHE6 is predominantly present in the early recycling endosome membranes, and is believed to have a role in regulating luminal pH and monovalent cation concentration in intracellular organelles [Brett et al., 2002; Nakamura et al., 2005]. Moreover, Roxrud et al. demonstrated that NHE6 in combination with NHE9 participated in regulation of endosomal pH in HeLa cells by means of the procedure of co-depletion of NHE6 and NHE9 [Roxrud et al. 2009], indicating the significant role of NHE6 in fine-tuning of endosomal pH in human cells. In the brain, exocytosis from recycling endosomes is essential for the growth of dendritic spines which grow during long-term potentiation (LTP). In the absence of recycling endosomal transport, spines are rapidly lost, and LTP stimuli fail to elicit spine growth [Park et al., 2006]. Thus, NHE6 has an important role in the growth of dendritic spines, and also in the development of normal brain wiring. Thus far, five *SLC9A6* mutations have been reported in six AS families; two nonsense mutations, one inframe deletion, one frameshift deletion, and one splicing mutation [Gilfillan et al., 2008; Schroer et al., 2010]. The precise pathogenesis by which these mutations produce disease remains to be clarified.

The aim of this study was to clarify the incidence and importance of *SLC9A6* mutations in AS-like patients and patients with XMR, and to shed light on the molecular pathogenesis of disease due to *SLC9A6* mutations.

MATERIALS AND METHODS

Enrolled Patients

We examined 22 affected Japanese males clinically suspected of having AS but who lacked the genetic abnormalities reported in AS (AS-like cohort). These patients had AS excluded by having negative results for the *SNURF-SNRPN* DNA methylation test (which identifies a deletion, uniparental disomy, or imprinting defect) and *UBE3A* mutation screening (performed as described previously) [Saitoh et al., 2005]. We also examined DNA samples from 104 Japanese patients suspected of having XMR (XMR cohort). The XMR samples were collected as a part of a project for the Japanese Mental Retardation Consortium [Takano et al., 2008]. This study was approved by the Institutional Review Board of Hokkaido University Graduate School of Medicine, and written informed consent was obtained from the parents of the enrolled patients.

Mutation Analysis of the *SLC9A6* Gene

We amplified each exon, including exon–intron boundaries, of the *SLC9A6* gene using polymerase chain reaction (PCR), and all amplicons were directly sequenced on an ABI 3130 DNA analyzer (Applied Biosystems, Foster City, CA) using BigDye Terminator V.1.1 Cycle Sequencing Kit (Applied Biosystems). *SLC9A6* encodes two alternatively spliced transcripts produced from alternative splicing donor sites in exon 2 which give rise to a long form designated as variant 1, and a short form called variant 2. Variant 1 and variant 2 code for NHE6.1 (isoform a) and NHE6.0 (isoform b), respectively (Fig. 1). The primers were designed to amplify each transcript variant. The primers sequence used for amplification and sequencing are available on request. Genomic DNA (10 ng) extracted from peripheral blood was amplified in a total PCR volume of 20 μl containing 1× buffer, 0.4 μM of each primer (forward/reverse), 0.18 mM dNTPs, 0.5 U AmpliTaq Gold® DNA Polymerase (Applied Biosystems). The PCRs for all exons except exon one were performed at 94°C for 10 min followed by 30 cycles of 94°C for 30 sec, 55°C for 30 sec, 72°C for 30 sec, then one cycle at 72°C for 7 min. The high CpG content of exon 1 required it to be amplified in a total reaction volume of 20 μl containing 1× buffer, 0.4 μM of each primer, 0.2 mM dNTPs, 0.4 U Phusion® Hot Start High-Fidelity DNA Polymerase (Finnzymes, Vantaa, Finland), and 3% DMSO. The thermocycling conditions for exon 1 were 98°C for 3 min followed by 35 cycles of 98°C for 10 sec, 65°C for 30 sec and 72°C for 30 sec and then one cycle of 72°C for 5 min. The PCR products were purified with Wizard® PCR Preps DNA Purification System (Promega, Madison, WI) prior to sequencing. All mutations are referred to in relation to reference sequence NM_001042537.

Cell Culture and Cycloheximide Treatment

Epstein–Barr virus (EBV)-transformed lymphoblastoid cells lines were established from peripheral blood cells using standard methods. To prevent potential degradation of transcripts containing premature translation termination codons (PTCs) by nonsense mediated mRNA decay (NMD), lymphoblastoid cells from the patient with the *SLC9A6* mutation and normal controls were treated with 100 μg/ml cycloheximide (CHX) (Sigma, St. Louis, MO). This compound interferes with NMD through inhibition of protein synthesis [Aznarez et al., 2007]. CHX or a 0.1% DMSO control vehicle was used 4 hr prior to RNA extraction from the cell lines [Carter et al., 1995].

RT-PCR

Total RNA from cultured lymphoblastoid cells from the patient and four normal controls, was extracted using the RNAqueous® Kit (Applied Biosystems). Reverse transcription was performed using 100 ng of total RNA and the High-Capacity cDNA Reverse Transcription Kit (Applied Biosystems) in a total reaction volume of 20 μl containing 1× Random primers, 4 mM dNTP mix, 2.5 U of Multiscribe™ Reverse Transcriptase, and 1 μl of RNase Inhibitor. The reactions were incubated at 25°C for 10 min, then at 37°C for 120 min and then followed by 85°C for 5 min to inactivate the reverse transcriptase. Complementary DNA was then amplified using a primer set designed to amplify exon 2–5; forward 5′-GTCTTTTGGTGGGCCTTGT-3′, reverse 5′-GTCCCGTTACC-TTCATCAG-3′. PCR products for NHE6.1 (transcript variant 1) and NHE6.0 (transcript variant 2) were 399 and 303 bp, respectively.

Real-Time Quantification of *SLC9A6* mRNA

To measure *SLC9A6* transcript variant 1 and variant 2, both of which are alternative splicing products, primers and TaqMan® MGB probes were designed with Primer® Express Software (Applied Biosystems; Fig. 1). The Primer and MGB probe sequence

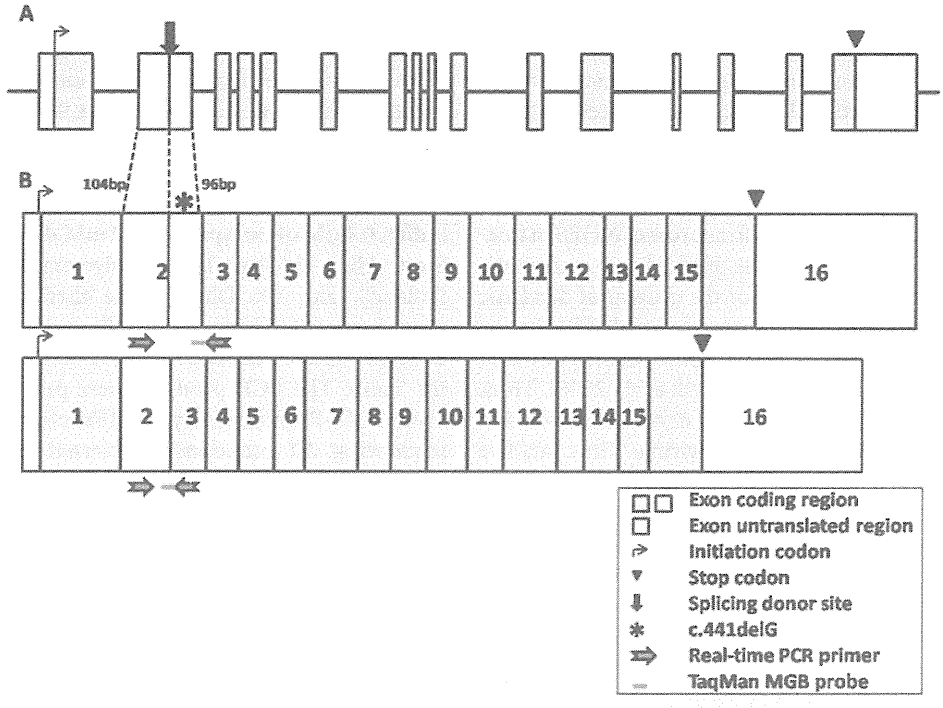

FIG. 1. A: Genomic structure of the *SLC9A6* gene. B: Two alternatively spliced transcripts of the *SLC9A6* gene. Above: *SLC9A6* transcript variant 1 (encodes NHE6.1 or isoform a). Below: *SLC9A6* transcript variant 2 (encodes NHE6.0 or isoform b). The location of the *SLC9A6* mutation in our patient is shown with *. Primers and probes used in real-time quantitative PCR are shown (horizontal arrows).

for variant 1 were forward primer 5′-TGAGTATATGCTG-AAAGGAGAGATTAGTTC-3′, reverse primer 5′-GATAGGA-GGAAGTAATATGTTGAAAAATACTTC-3′, TaqMan MGB probe 5′-CTTAGAAAGGTTACTTTTGATCC-3′; and for variant 2 forward primer 5′-CTGTGAAGTGCAGTCAAGTCCAA-3′, reverse primer 5′-GATAGGAGGAAGTAATATGTTGAAAAA-TACTT-3′, TaqMan MGB probe 5′-CTACCTTACTGGTTA-CTTTTGA-3′. Human *GAPDH* MGB probe and primers purchased from Applied Biosystems were used as the internal control. Patient cDNA was transcribed from 10 ng of total RNA in a total volume of 25 µl containing 1× TaqMan® Universal PCR Master Mix (Applied Biosystems), 0.9 µM of each primer (sense/antisense) and 0.25 µM of probe. Thermocycling was 95°C for 10 min, followed by 40 cycles of 95°C for 15 sec and 60°C for 1 min. Real-time quantitative PCR was performed using the ABI PRISM 7700 (Applied Biosystems). The $2^{-\Delta\Delta Ct}$ method was used for relative quantification.

Western Blot Analysis

HeLa cells and cultured lymphoblastoid cells from the patient, mother and normal controls were washed with phosphate buffered saline and suspended in lysis buffer (phosphate buffered saline containing 1% Triton-X, 1 µg/ml aprotinin, 1 µg/ml pepstatin A, and 1 µg/ml leupeptin). HeLa cells expressing the NHE6.1 were used as a control. The cells were disrupted by sonication and centrifuged at 20,000*g* for 10 min at 4°C. The supernatants were then resolved by SDS-polyacrylamide electrophoresis and transferred to polyvinylidene fluoride membrane (Millipore, Billerica, MA). NHE6 was detected with rabbit polyclonal anti-NHE6 antibody [Ohgaki et al., 2008], anti-rabbit IgG antibody conjugated with horseradish peroxidase (Vector Laboratories, Burlingame, CA) and chemiluminescence reagent (ECL Western Blotting Detection System; GE Healthcare, Waukesha, WI).

RESULTS

Identification of a *SLC9A6* Mutation

We identified only one male patient with a frameshift mutation (c.441delG, p.S147fs) in exon 2, out of 22 male patients in the AS-like cohort (Fig. 2). This frameshift mutation causes a PTC. His healthy mother was heterozygous for the mutation.

No mutation in the *SLC9A6* gene was identified in the XMR cohort. However, two common polymorphisms (rs2291639, rs2307131), and one putative novel polymorphism in intron 12 (c.1692 +10 A>G) were detected.

Clinical Features of the Patient With the *SLC9A6* Mutation

The affected male patient at birth suffered from mild neonatal asphyxia, however he had no other perinatal problems. His parents

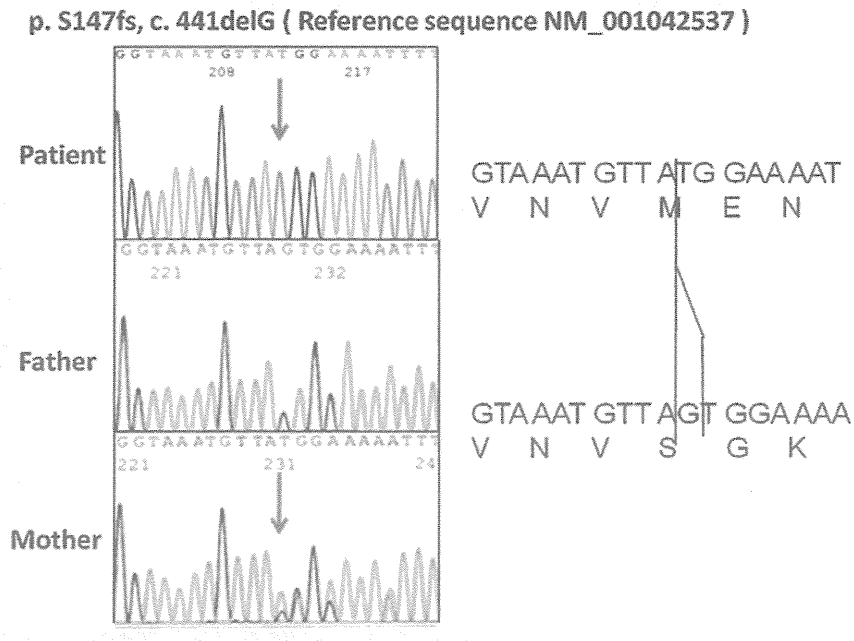

FIG. 2. Chromatographs showing the *SLC9A6* mutation in our patient, and the equivalent genomic region in both his parents. The mutation c.441delG is located in exon 2 and is only present in transcript variant 1. His mother was heterozygous for this mutation, while his father did not have the mutation. This mutant transcript leads to premature protein truncation. The mutation is described relative to reference sequence NM_001043537. [Color figure can be seen in the online version of this article, available at http://onlinelibrary.wiley.com/journal/10.1002/(ISSN)1552-485X]

were non-consanguineous and he did not have any family history of neurological diseases. Although formal clinical assessment was not conducted to the mother, she is healthy and does not have intellectual disability. His clinical features are summarized in Table I. He showed typical findings of AS; severe developmental delay with absence of verbal language, generalized hypotonia, easily provoked laughter, epilepsy, ataxia, strabismus, and microcephaly. His occipitofrontal head circumference at birth was 33.8 cm (+0.4 SD), but his head growth has decelerated into 51.5 cm (−3.0 SD) at 18 years of age. He acquired head control at three months of age, sat and crawled at 6 months of age, and walked unassisted at 18 months of age. His first epileptic attack occurred at 4 years of age. After this first attack, he lost his ability to walk until he was 5 years old. His epileptic attacks consisted of multiple types of seizures, and they were difficult to control with ACTH or several anti-epileptic drugs. TRH treatment improved his awakening and activity levels, and he transiently acquired the ability to walk. However, subsequently his ability to walk was lost, probably due to exacerbation of ataxia. His deep tendon reflex was not increased and no other features of spasticity or peripheral neuropathy were identified. His EEG findings included a background frequency of 5–6 Hz theta waves and spontaneous appearance of 3 Hz diffuse high voltage slow waves. TRH did not change the frequency of his seizures or his EEG findings. He showed no cerebellar atrophy on magnetic resonance imaging (MRI) at 5 years of age. MRS was not performed. He had a normal G-banding karyotype.

Downregulation of the *SLC9A6* Variant 1 in the Patient With the Mutation

The identified mutation c.441delG is located in exon 2 and is only present in variant 1 (Fig. 1). Therefore, the mutation only affects NHE6.1, leaving NHE6.0 intact. Reverse transcriptase PCR demonstrated that *SLC9A6* variant 1 mRNA expression decreased in our patient (Fig. 3A) compared to that in four normal controls. On the other hand, variant 2 expression was increased in the patient compared to the controls. To further investigate mutant *SLC9A6* gene expression, real-time quantitative PCR (qPCR) was performed using cDNA from the patient and normal controls. Quantitative PCR confirmed that *SLC9A6* variant 1 was significantly downregulated in the patient, while it was not downregulated in normal controls (Fig. 4A). Furthermore, the *SLC9A6* variant 2 mRNA in the patient was significantly increased compared to normal controls (Fig. 4B).

Nonsense Mediated Decay Was Involved in the Downregulation of Mutant *SLC9A6* in the Patient

To investigate the possible involvement of NMD in the downregulation of mutant *SLC9A6* in the patient's lymphoblastoid cells, we treated the cells with CHX. After CHX treatment, the expression level of *SLC9A6* variant 1 increased compared to normal control samples on RT-PCR (Fig. 3B). It was also proved that the expression level of variant 1 was significantly increased by performing qPCR, while the expression level in normal control samples

TABLE I. Clinical Findings in Affected Males Previously Reported and Our Patient

Family number: report affected males number (examined number)	1: Gilfillan et al. [2008] 3 (3)	2: Gilfillan et al. [2008] 2 (1)	3: Gilfillan et al. [2008] 3 (3)	4: Gilfillan et al. [2008], Christianson et al. [1999] 16 (4)	5: Schroer et al. [2010] 6 (6)	6: Schroer et al. [2010] 1 (1)	Our patient
Development and behavior							
Profound delay	+	+	+	+	+	+	+
Verbal language absent	+	+	+	+	+	+	+
Easily provoked laughter	+	+	+	+	3/6	−	+
CNS findings							
Epilepsy	+	+	+	+	+	+	+
Ataxia	+	+	+	+	NR	NR	+
Hyperkinetic movements	2/3	−	+	−	2/6	NR	−
Strabismus	+	+	+	+	5/6	+	+
Physical findings							
Microcephaly	+	+	+	3/4	5/6	+	+
Open mouth + drooling	2/3	+	+	NR	4/6	+	+
Swallowing difficulty	2/3	+	1/3	1/4	NR	+	−
Flexed arms	+	NR	1/3	+	3/6	−	−
Electroencephalography							
Epileptiform activity	+	+	+	+	+	+	+
Background activity	10–11 Hz	1.5–3 Hz	4–7 Hz	3–6 Hz to 11–14 Hz	NR	α rhythm	5–6 Hz
Brain MRI/autopsy							
Cerebellar atrophy	1/3	NR	NR	2/4	2/6	+	−
Mutation	p.E287_S288del c.936_941delAAAGTG	p.R500X c.1574C → T	p.V176_201del c.679 +1 delGTAA	p.H203fs c.684_685delAT	p.R500X c.1574C → T	p.Q437X c.1391C → T	p.S147fs c.441delG

+, present with all the patients; −, not present; NR, not recorded.

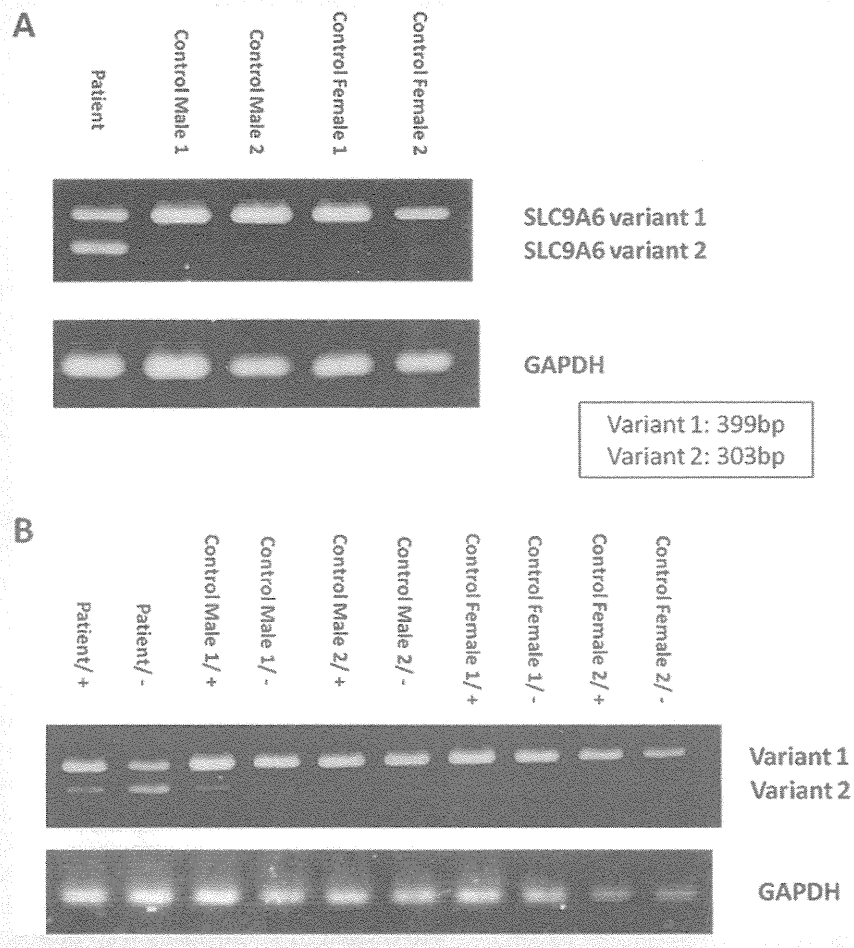

FIG. 3. RT-PCR amplification of the *SLC9A6* gene. A: *SLC9A6* variant 1 mRNA expression was decreased in the patient compared to that in four normal controls. On the other hand, variant 2 expression was increased in the patient compared to that in the controls. B: CHX treatment increases the mutant *SLC9A6* variant 1 mRNA expression, leading to similar expression levels in the patient and four normal controls samples. (+) After CHX treatment, (−) no CHX treatment.

was unchanged (Fig. 4A). The expression level of *SLC9A6* variant 2 increased in all samples after CHX treatment, however the increase was significant only in control samples (Fig. 4B).

Decreased Expression of the NHE6 Protein From Mutant *SLC9A6*

Western blotting was performed to investigate expression of the NHE6 protein in the homogenate of lymphoblastoid cell lines from the patient and his mother. As a result, protein expression of NHE6.1 was not detected in the patient (Fig. 5A,B). The same NHE6.1 was detected in HeLa cells and cells from the patient's mother as well as in the controls. NHE6.0, which was expected to be 10–20 kDa smaller than NHE6.1on SDS–PAGE [Ohgaki et al., 2008], was not detected in any sample (Fig. 5B).

DISCUSSION

In this study we investigated 22 male AS-like patients and 104 male patients with XMR, and identified only one AS-like patient with a *SLC9A6* frameshift mutation. This result further confirms *SLC9A6* is not a major cause of AS-like cases, as reported by Fichou et al. [2009]. Although the number of patients with XMR in this study was small, *SLC9A6* is likely to account for only small proportion of XMR cases.

Patients with *SLC9A6* mutations reported by Gilfillan et al., exhibit cardinal features similar to those of AS including severe developmental delay, mental retardation with absent or minimal use of words, easily provoked laughter, ataxia, epilepsy, hyperkinetic movement, nystagmus, and microcephaly.

Gilfillan et al. also identified possible features of difference between these patients and AS patients, including slow progression of symptoms, thin body, cerebellar atrophy, increased glutamate/

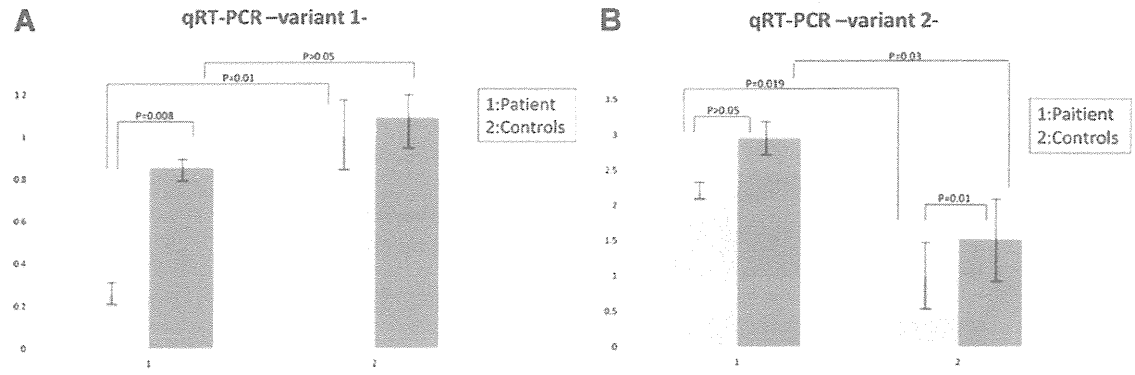

FIG. 4. Real-time quantitative PCR in samples from cell lines from the patient and four normal controls containing two males and two females. The light gray bars indicate the expression levels of *SLC9A6* before CHX treatment, while deep gray bars after CHX treatment. We performed statistical analysis using paired and unpaired Student's t-test. Error bars show standard deviation. A: The *SLC9A6* variant 1 was significantly downregulated in samples from the patient while it was not downregulated in samples from four normal controls. After CHX treatment, expression level of the *SLC9A6* variant 1 mRNA in the patient's sample was significantly increased. B: The *SLC9A6* variant 2 in the patient's sample was significantly increased compared to normal controls. Expression level of *SLC9A6* variant 2 increased in all samples after CHX treatment, but a significant increase was only seen in samples from controls.

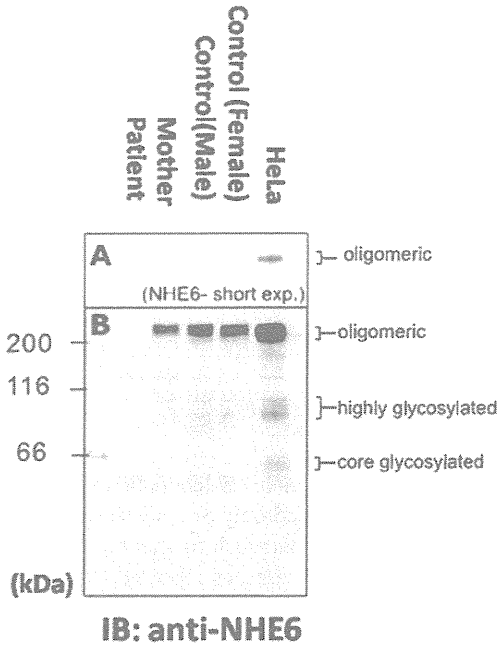

FIG. 5. Protein expression of NHE6 in cultured lymphoblastoid cells and HeLa cells. In the patient, no protein expression of NHE6 isoforms was detected with Western blotting using anti-NHE6 antibody. A: A cropped image taken using a short exposure time demonstrating the oligomeric form of NHE6. Protein size in kDa is shown by numbers on the left of the image. B: A chemiluminescence image of Western blotting taken with a longer exposure time.

glutamic acid peak on MRS, and rapid frequency of 10–14 Hz waves on EEG (Table I). Our patient lost his ability to walk although he did not demonstrate spasticity, demonstrating a slowly progressive clinical course consistent with findings in Gilfillan's report. Indeed, slow progression may be a distinctive clinical feature for patients with *SLC9A6* mutations. One of the families which Gilfillan et al. investigated was previously reported by Christianson et al. [1999], and designated as Christianson syndrome. Schroer et al. reported patients with Christianson syndrome, and they showed that the patients demonstrated an AS-like phenotype. However, while the clinical features of our patient were consistent with those of most patients previously reported by Gilfillan, there were differences including the EEG findings and lack of cerebellar atrophy. Despite this, our patient did meet the diagnostic criteria for AS [Williams et al., 2006]. Therefore, this study further demonstrated that a patient with a *SLC9A6* mutation may resemble patients with AS. Further, this striking similarity between patients with AS and those with *SLC9A6* mutations suggests a possible relationship between the gene function of *UBE3A* and *SLC9A6* in the developing brain.

Our patient's mutation created a frameshift resulting in 7 missense amino acids followed by a stop codon. This mutation was present only in *SLC9A6* transcript variant 1. *SLC9A6* mRNA has two transcript variants caused by alternative splicing in exon 2 (Fig. 1), but the role of each variant has not been clarified. The mutation detected in our patient only affects variant 1 sequence, but the phenotype of the patient was as severe as those in previously reported patients. Therefore, our finding suggests that the NHE6.1 plays an important role in brain function.

Nonsense mediated decay is involved in regulating the expression of alternatively spliced forms containing PTCs [Lareau et al., 2007; Ni et al., 2007]. Since the identified mutation was predicted to result in a PTC, we speculated that NMD could be involved in disease pathogenesis. The result of qRT-PCR showed a significant

decrease in *SLC9A6* variant 1 mRNA expression in the patient sample. This reduction was restored by CHX treatment, while *SLC9A6* variant 1 expression was unaltered by CHX treatment in normal control samples. Expression of *SLC9A6* variant 2 in the patient on the other hand, was significantly increased compared to that in control samples, however it was not influenced by CHX treatment. Therefore, the c.441delG mutation in the patient seems to have modified the alternative splicing pattern, leading to an increase in variant 2 expression. Alternatively, low variant 1 could trigger a regulatory feed back on transcription causing the apparent increase in variant 2 expression. A mutation causing premature protein truncation could alter the splicing pattern and lead to exon skipping, use of alternative splice sites, and intron retention [Hentze and Kulozik, 1999; Mendell and Dietz, 2001]. Our results indicated that the c.441delG mutation caused a PTC altered the splicing pattern, and activated NMD machinery then downregulated *SLC9A6* variant 1 expression.

As protein NHE6.1 was not detected, this indicates an absence of intact NHE6.1. NHE6.0 was also not detected. These findings conclusively indicated that the identified mutation should cause total loss-of-function. Recently, Garbern et al. identified cases with an in-frame deletion of three amino acids, who showed milder dysmorphic features and higher gross motor abilities than those in cases previously reported [Garbern et al., 2010]. Their in-frame deletion should not cause total loss-of-function but create a mildly dysfunctional protein. Therefore, severe phenotypes including severe developmental delay and progressive neurological deterioration may be caused by truncated mutations and less severe phenotypes may be caused by missense or in-frame mutations, and such mild phenotypes are likely missed in patients with mild developmental delay.

Given that the *SLC9A6* variant 2 was upregulated, we speculated that upregulated variant 2 might partially compensate for the absence of NHE6.1. However, we could not establish the upregulation of the NHE6.0 protein, rather it was not detected in the patient's lymphoblastoid cells. NHE6.0 may be unstable compared to NHE6.1. Alternately, NHE6.0 translation may be inhibited. Further investigation is required to definitively answer this question.

NHE6 is found in the membranes of early recycling endosomes and transiently in plasma membranes. Its distribution is regulated by RACK1 [Ohgaki et al., 2008]. Recycling endosomal trafficking is essential for the growth of dendritic spines during LTP in the brain [Park et al., 2006]. The function of the protein product of *UBE3A*, E3 ubiquitin ligase, is also associated with dendritic spine morphology. Mice with a maternal null mutation in *Ube3a* are also reported to have defects in LTP, and manifest motor and behavioral abnormalities [Jiang et al., 1998]. In a recent study, *Ube3a* deficient mice demonstrated dendritic spine dysmorphology [Dindot et al., 2008]. Thus, *UBE3A* and *SLC9A6* could interact in a common pathway involved in dendritic spine development, with a mutation in either leading to an AS-like phenotype.

ACKNOWLEDGMENTS

The authors thank Dr. Tadashi Ariga for critical reading of the manuscript.

REFERENCES

Aznarez I, Zielenski J, Rommens JM, Blencowe BJ, Tsui LC. 2007. Exon skipping through the creation of a putative exonic splicing silencer as a consequence of the cystic fibrosis mutation R533X. J Med Genet 44: 341–346.

Brett CL, Wei Y, Donowitz M, Rao R. 2002. Human Na(+)/H(+) exchanger isoform 6 is found in recycling endosomes of cells, not in mitochondria. Am J Cell Physiol 5:1031–1041.

Carter MS, Doskow J, Morris P, Li S, Nhim RP, Sandstedt S, Wilkinson MF. 1995. A regulatory mechanism that detects premature nonsense codons in T-cell receptor transcripts in vivo is reversed by protein synthesis inhibitors in vitro. J Biol Chem 270:28995–29003.

Christianson AL, Stevenson RE, van der Meyden CH, Pelser J, Theron FW, van Rensburg PL, Chandler M, Schwartz CE. 1999. X linked severe mental retardation, craniofacial dysmorphology, epilepsy, ophthalmoplegia, and cerebellar atrophy in a large South African kindred in localized to Xq24–q27. J Med Genet 36:759–766.

Dindot SV, Antalffy BA, Bhattacharjee MB, Beaudet AL. 2008. The Angelman syndrome ubiquitin ligase localizes to the synapse and nucleus, and maternal deficiency results in abnormal dendritic spine morphology. Hum Mol Genet 17:111–118.

Fichou Y, Bahi-Buisson N, Nectoux J, Chelly J, Heron D, Cuisset L, Bienvenu T. 2009. Mutation in the *SLC9A6* gene is not a frequent cause of sporadic Angelman-like syndrome. Eur J Hum Genet 17:1378–1380.

Garbern JY, Neumann M, Trojanowski JQ, Lee VM, Feldman G, Norris JW, Friez MJ, Schwartz CE, Stevenson R, Sima AA. 2010. A mutation affecting the sodium/proton exchanger, *SLC9A6*, causes mental retardation with tau deposition. Brain 133:1391–1402.

Gilfillan GD, Selmer KK, Roxrud I, Smith R, Kyllerman M, Eiklid K, Kroken M, Mattingsdal M, Egeland T, Stenmark H, Sjoholm H, Server A, Samuelsson L, Christianson A, Tarpey P, Whibley A, Stratton MR, Futreal A, Teague J, Edkins S, Gecz J, Turner G, Raymond FL, Schwartz C, Stevenson RE, Undlien DE, Stromme P. 2008. *SLC9A6* mutations cause X-linked mental retardation, microcephaly, epilepsy, and ataxia, a phenotype mimicking Angelman Syndrome. Am J Hum Genet 82: 1003–1010.

Hentze MW, Kulozik AE. 1999. A perfect message: RNA surveillance and nonsense-mediated decay. Cell 96:307–310.

Jiang YH, Armstrong D, Albrecht U, Atkins CM, Noebels JI, Eichele G, Sweatt JD, Beaudet AL. 1998. Mutation of the Angelman ubiquitin ligase in mice causes increased cytoplasmic p53 and deficits of contextual learning and long-term potentiation. Neuron 21:799–811.

Lareau LF, Inada M, Green RE, Wengrod JC, Brenner SE. 2007. Unproductive splicing of SR genes associated with highly conserved and ultraconserved DNA elements. Nature 446:926–929.

Mendell JT, Dietz HC. 2001. When the message goes awry: Disease-producing mutations that influence mRNA content and performance. Cell 107:411–414.

Nakamura N, Tanaka S, Teko Y, Mitsui K, Kanazawa H. 2005. Four Na^+/H^+ exchanger isoforms are distributed to Golgi and post-Golgi compartments and are involved in organelle pH regulation. J Biol Chem 280:1561–1572.

Ni JZ, Grate L, Donohue JP, Preston C, Nobida N, O'Brien G, Shiue L, Clark TA, Blume JE, Ares M, Jr. 2007. Ultraconserved elements are associated with homeostatic control of splicing regulators by alternative splicing and nonsense-mediated decay. Genes Dev 21:708–718.

Ohgaki R, Fukura N, Matsushita M, Mitsui K, Kanazawa H. 2008. Cell surface levels of organellar Na^+/H^+ exchanger isoform 6 are regulated by interaction with RACK1. J Biol Chem 283:4417–4429.

Park M, Salgado JM, Ostroff L, Helton TD, Robinson CG, Harris KM, Ehlers MD. 2006. Plasticity-induced growth of dendritic spines by exocytic trafficking from recycling endosomes. Neuron 52:817–830.

Roxrud I, Raiborga C, Gilfillan GD, Strømmed P, Stenmark H. 2009. Dual degradation mechanisms ensure disposal of NHE6 mutant protein associated with neurological disease. Exp Cell Res 135:3014–3027.

Saitoh S, Wada T, Okajima M, Takano K, Sudo A, Niikawa N. 2005. Uniparental disomy and imprinting defects in Japanese patients with Angelman syndrome. Brain Dev 27:389–391.

Schroer RJ, Holden KR, Tarpey PS, Matheus MG, Griesemer DA, Friez MJ, Fan JZ, Simensen RJ, Stromme P, Stevenson RE, Stratton MR, Schwartz CE. 2010. Natural history of Christianson syndrome. Am J Med Genet Part A 152A:2775–2783.

Takano K, Nakagawa E, Inoue K, Kamada F, Kure S, Goto Y, Japanese Mental Retardation Consortium. 2008. A loss-of-function mutation in the FTSJ1 gene causes nonsyndromic X-linked mental retardation in a Japanese family. Am J Med Genet Part B 147B:479–484.

Williams CA, Beaudet AL, Clayton-Smith J, Knoll JH, Kyllerman M, Laan LA, Magenis RE, Moncla A, Schinzel AA, Summers JA, Wagstaff J. 2006. Angelman Syndrome 2005: Updated consensus for diagnostic criteria. Am J Med Genet Part A 140A:413–418.

見逃してはいけない家族性腫瘍：本邦における母斑基底細胞癌症候群の遺伝子変異と臨床的特徴

宮下俊之　桐生麻衣子　齋藤加代子　杉田克生
遠藤真美子　藤井克則

家族性腫瘍　第11巻　第1号　別刷
2011年1月発行

見逃してはいけない家族性腫瘍：本邦における母斑基底細胞癌症候群の遺伝子変異と臨床的特徴

宮下俊之[*1]　桐生麻衣子[*1]　齋藤加代子[*2]　杉田克生[*3]
遠藤真美子[*4]　藤井克則[*4]

母斑基底細胞癌症候群（NBCCS，Gorlin 症候群）は骨格を中心とする小奇形と高発癌を特徴とする常染色体性優性遺伝疾患である．今回行った全国調査で311例のNBCCS患者が報告された．欧米の報告と比べて基底細胞癌の発症率が低く（38%），発症年齢も高い（37.5歳）点が注目された．また，現在までに行った35家系における責任遺伝子 *PTCH1* の解析の結果，32家系（91%）で遺伝子欠失（5家系）を含む何らかの遺伝子異常が検出された．

キーワード：癌抑制遺伝子，*PTCH1*，基底細胞癌，角化嚢胞性歯原性腫瘍，ヘッジホッグシグナル，半量不全

I.　母斑基底細胞癌症候群とは

母斑基底細胞癌症候群（nevoid basal cell carcinoma syndrome; NBCCS）は骨格を中心とする小奇形と高発癌を特徴とする常染色体性優性遺伝疾患であり，Gorlin と Goltz によって1960年に報告された[1]．発見者の名前をとって Gorlin 症候群，または Gorlin-Goltz 症候群とも呼ばれる．更に基底細胞母斑症候群（basal cell nevus syndrome）と呼ばれることもある．臨床診断基準は細部が若干異なる Evans らによるものと Kimonis らによるものが報告されているが，後者を表1に示した[2]．本邦における発生頻度は明らかでないが，英国では26,000人に1人という報告がある．

責任遺伝子は分泌型タンパク質であるソニックヘッジホッグ（Shh）の抑制性受容体をコードする *PTCH1* である[3,4]．*PTCH1* の半量不全による Shh シグナル伝達の亢進が発症機序と考えられる．哺乳類には *PTCH1* と相同性の高い *PTCH2* が存在する．*PTCH2* に変異のある NBCCS の1家系が報告されている[5]が，*PTCH2* のノックアウトマウスで表現型が現れない点，変異の種類がミスセンス変異である点から，この変異が本当に NBCCS の発症に関与していると結論づけるには，更なる症例報告が必要と思われる．更に最近，*PTCH1* の下流で Shh シグナル伝達を抑制している *SUFU* 遺伝子にスプライシング変異のある NBCCS の1家系が報告された[6]．

II.　本邦における母斑基底細胞癌症候群の臨床的特徴

我々は厚生労働科学研究費補助金・難治性疾患克服研究事業の一環として NBCCS の全国調査を行った．詳細は別途報告の予定であるため，本稿ではその概略と腫瘍の発生に関して速報として述べるに留めたい．また最終の集計で若干数字が異なってくる可能性もある．

一次調査の結果，147施設から311症例の報告があった．Kimonis らの診断基準にあげられている各表現型の頻度を表1の括弧内に示した．大症状はすべて1/3以上の症例で認められた．家族歴陽性例は40%であるため，半数以上の症例は新規の遺伝子変異と考えられた．

NBCCS 症例に発症した腫瘍を海外の報告と比較してまとめたのが表2である．発症頻度が最も高い腫瘍は，顎骨に生ずる角化嚢胞性歯原性腫瘍（keratocystic odontogenic tumor; KCOT）である．KCOT は歯原性角化嚢胞（odontogenic keratocyst; OKC）として嚢胞に分類されていたが，浸潤性や再発率の高さ，増殖活性の高さから2005年の WHO 分類により腫瘍として取り扱うようになった[7]．孤発例に比べ NBCCS に伴う KCOT は多発する傾向があり，再発率も高いといわれている．

NBCCS における基底細胞癌（basal cell carcinoma; BCC）の発症は疾患名からもわかるように有名であり，白人では天寿を全うする間には必ず発症すると言われているほど頻度が高い．しかしながら表に示すように日本人では明らかに欧米の報告より頻度が低く（38% vs. 76～80%），かつ平均発症年齢も高い傾向が認められた（37.4

[*1] 北里大学医学部分子遺伝学
[*2] 東京女子医科大学附属遺伝子医療センター
[*3] 千葉大学教育学部基礎医科学
[*4] 千葉大学大学院医学研究院小児病態学
連絡先：宮下俊之　〒252-0374　相模原市南区北里1-15-1
北里大学医学部分子遺伝学
Tel：042-778-8816　Fax：042-778-9214
2010年11月18日受理
家族性腫瘍 第11巻 第1号（2011年）p.14-18

歳 vs. 20.3～21.4歳）．症例数は少ないものの，韓国人でも同様の傾向が認められる[8]．これは皮膚癌全般に白人で発生頻度が高いという事実と一致する結果である．

表1．Kimonisらによる NBCCS の診断基準と出現率

大症状2つ，あるいは大症状1つと小症状2つを満たす場合 NBCCS と診断

大症状
1. 2個以上，あるいは20歳以下の基底細胞癌[38％]
2. 顎骨の歯原性角化嚢胞[86％]
3. 3個以上の手掌，足底の小陥凹[60％]
4. 大脳鎌の石灰化[79％]
5. 肋骨異常（二分肋骨，癒合あるいは極端な扁平化等）[36％]
6. 第一度近親（親，子，同胞，二卵性双生児）にNBCCSをもつ[40％]

小症状
1. 大頭症（身長で補正後）[27％]
2. 先天奇形（口唇口蓋裂[8％]，前頭突出[47％]，粗野顔貌[37％]，両眼開離[69％]）
3. その他の骨格異常（Sprengel変形[3％]，胸郭変形[7％]，合指症[2％]）
4. X線検査の異常：トルコ鞍骨性架橋[24％]，脊椎の異常（半椎等）[15％]，手足のモデリング欠損，手足の火焔様透亮像[3％]
5. 卵巣線維腫[4％]
6. 髄芽腫[3％]

文献2）による．[ ]内の数字は今回の全国調査における出現頻度．

生命予後の悪い髄芽腫の発生も有名であるが，日本人でも頻度は低かった．そのほかにも，頻度は低いものの，さまざまな腫瘍の合併がみられたが，偶然の合併も含まれているかもしれない．

III. 本邦における母斑基底細胞癌症候群の遺伝子変異

NBCCSの責任遺伝子 *PTCH1* は24個のエキソンからなり，ゲノム上の約73 kbにわたる遺伝子で，アミノ酸1,447個からなるタンパク質をコードしている．我々は現在までにNBCCSの35家系，41症例について遺伝子解析を行ってきた．*PTCH1* 全コーディングエキソンの塩基配列をPCR－シークエンス法で解析したところ27家系（77％）で全て異なる変異が検出された（図1）．変異の内訳は1～4塩基の欠失，挿入によるフレームシフト変異が15家系（43％）で最も多かった．変異が認められた場所を図2に示した．エキソン2からエキソン20まで満遍なく変異が認められ，変異のホットスポットは見られなかった．これらの所見は欧米の報告と大差ないものである．しかしながら4家系で見出されたミスセンス変異は膜貫通領域に集中しており，この部分はPTCH1タンパク質の機能に重要な役割を演じていることが示唆される（図3）．また最も3′側ではエキソン20にフレームシフト変異がみられることより，PTCH1タンパク質のC末端側約300個のアミノ酸が欠失すると機能が失われることが示唆される．

表2．主な腫瘍とその発生頻度

腫　瘍	報告者（国）	度数（あり/全体）	頻度（％）	平均発症年齢
Basal cell carcinoma				
	本研究（日本）	56 / 148	38	37.4
	Kimonis（米国）	71 / 90	80	21.4
	Evans（英国）	＞20 years 33 / 45	73	
		＞40 years 19 / 21	90	
	Shanley（オーストラリア）	90 / 118	76	20.3
	Ahn（韓国）	5 / 33	15.2	
Keratocystic odontogenic tumor				
	本研究（日本）	126 / 146	86.3	19.8
	Kimonis（米国）	78 / 105	74	17.3
	Evans（英国）	46 / 70	66	
	Shanley（オーストラリア）	85 / 113	75	15.5
	Ahn（韓国）	30 / 33	91	
Medulloblastoma				
	本研究（日本）	4 / 120	3.3	0～4
	Kimonis（米国）	4 / 105	4	2～3
	Evans（英国）	3 / 84	4	1～4
	Shanley（オーストラリア）	1 / 118	1	
	Ahn（韓国）	1 / 33	3	
Ovarian fibroma				
	本研究（日本）	5 / 40	12.5	20.8
	Kimonis（米国）	9 / 52	17	
	Evans（英国）	6 / 25	24	
	Shanley（オーストラリア）	9 / 63	14	
	Ahn（韓国）	1 / 33	3	

上記の他に頻度の少ない腫瘍として髄膜腫（4例），その他の卵巣腫瘍（3例），心臓線維腫（2例），甲状腺腫瘍（2例）があった．国外の頻度は文献2，8，14，15）によった．KimonisらによるBCCのデータは白人に限った値である．

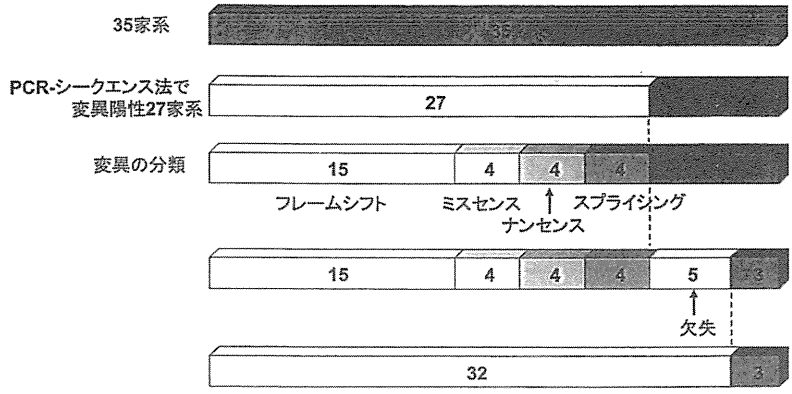

図1．NBCCSの*PTCH1*遺伝子解析．

全35家系を解析し，PCR－シークエンス法で27家系が変異陽性であった．この時点で変異陰性であった残る8家系のうち5家系で*PTCH1*遺伝子の欠失が認められたため，結局32/35＝91％で何らかの変異が見出された．

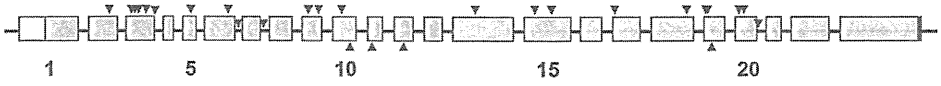

図2．遺伝子変異の分布．

*PTCH1*遺伝子の各エキソン（四角）と検出された27の変異の位置（矢頭）を示した．翻訳領域は灰色で，非翻訳領域は白で表した．イントロンの長さは実際より短く表されている．エキソン24は3′非翻訳領域なので省略した．遺伝子欠失の5家系は含まれていない．ミスセンス変異は上向きの矢頭で，その他の変異は下向きの矢頭で表した．

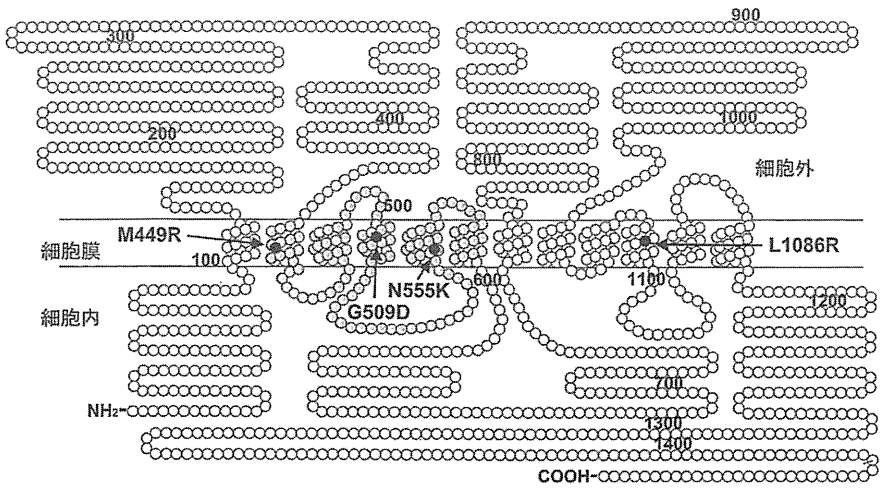

図3．ミスセンス変異の分布．

*PTCH1*タンパク質の構造を模式的に示した．数字はアミノ末端から数えたアミノ酸の番号を示す．我々が見出したミスセンス変異を黒丸で，ステロールセンシングドメインと呼ばれるいくつかのタンパク質で保存されている領域を灰色の丸で表した．

従来，通常行われる遺伝子解析で変異陰性であった複数のNBCCS症例に対して，積極的にコピー数解析を行った報告はない．我々はこの時点で変異陰性であった8家系につき，*PTCH1*の遺伝子欠失の可能性を疑い，高密度オリゴヌクレオチドマイクロアレイを用いてコピー数解析を行ったところ，5家系（全家系の14％）で*PTCH1*遺伝子の半量欠失を検出できた（図1）[9]．欠失の範囲は最も小さいもので165 kbであり，この欠失に含まれる遺伝子は*PTCH1*のみであった．この症例はNBCCSが*PTCH1*の半量不全で発症することを証明する貴重な症例であった．欠失は大きなもので11 Mbに及んでおり，*PTCH1*遺伝子を含む複数の遺伝子が欠失しており，痙攣や重度の精神運動発達遅滞等，NBCCSでは通常出現しない所見が認められた．結局，コピー数解析まで行っても遺伝子異常が見出されなかった家系は3家系であり，遺伝子異常の検出率は91％と，従来のいずれの報告より高いものであった．

IV．　まとめと今後の展望

本邦における母斑基底細胞癌症候群の遺伝子変異と臨床的特徴について概説した．今回行った全国規模のアンケート調査によって，日本人のNBCCSでは白人と比べBCCの発症が明らかに少なく，かつ発症年齢も高いことが明らかとなった．また，本症を扱う診療科は，症例数の多い順

に歯科，皮膚科，小児科，脳外科と多岐にわたることも明らかとなった．多臓器に病変が生じる本症の診療にあたっては，各診療科の密接な連携が重要であると思われた．

NBCCSには年齢とともに出現する症状が少なくない．また髄芽腫は早期発見が重要であるうえ，NBCCS患者は放射線感受性が高く，放射線照射域に一致して，後に多数の基底細胞癌やその他の二次癌を生じるため，放射線療法は禁忌，あるいは最小限に留めるべきであるとする報告がある[10-12]．したがって若年発症の髄芽腫（特にdesmoplastic subtype）の症例はNBCCSである可能性を慎重に検討する必要がある．また基底細胞癌は不必要な紫外線照射を避けることである程度予防可能である．以上の点を考慮すると，遺伝子診断は小児においても治療，経過観察にとってメリットが大きいと考えられる．患者の子供で親の変異がないとわかれば安心して日光を浴びることもできるし，不要な検査を省くことも可能である．また，臨床的にNBCCSであって通常の遺伝子解析で変異陰性の結果がでた場合は，遺伝子欠失の可能性が高いので，定量PCR，multiplex ligation-dependent probe amplification (MLPA) 法，あるいはマイクロアレイ法等によるコピー数解析を推奨したい．

最近，Shhシグナル伝達を抑制する分子標的薬の開発が盛んであり，一部臨床応用も始まっている[13]．将来NBCCSに発症する各種腫瘍にも応用されることを期待したい．

文　献

1) Gorlin RJ, Goltz RW : Multiple nevoid basal-cell epithelioma, jaw cysts and bifid rib : a syndrome. N Engl J Med 1960 ; 262 : 908−912.
2) Kimonis VE, Goldstein AM, Pastakia B, et al. : Clinical manifestations in 105 persons with nevoid basal cell carcinoma syndrome. Am J Med Genet 1997 ; 69 : 299−308.
3) Hahn H, Wicking C, Zaphiropoulous PG, et al. : Mutations of the human homolog of Drosophila *patched* in the nevoid basal cell carcinoma syndrome. Cell 1996 ; 85 : 841−851.
4) Johnson RL, Rothman AL, Xie J, et al. : Human homolog of *patched*, a candidate gene for the basal cell nevus syndrome. Science 1996 ; 272 : 1668−1671.
5) Fan Z, Li J, Du J, et al. : A missense mutation in PTCH2 underlies dominantly inherited NBCCS in a Chinese family. J Med Genet 2008 ; 45 : 303−308.
6) Pastorino L, Ghiorzo P, Nasti S, et al. : Identification of a SUFU germline mutation in a family with Gorlin syndrome. Am J Med Genet A 2009 ; 149A : 1539−1543.
7) Madras J, Lapointe H : Keratocystic odontogenic tumour: reclassification of the odontogenic keratocyst from cyst to tumour. J Can Dent Assoc 2008 ; 74 : 165−165h.
8) Ahn SG, Lim YS, Kim DK, et al. : Nevoid basal cell carcinoma syndrome: a retrospective analysis of 33 affected Korean individuals. Int J Oral Maxillofac Surg 2004 ; 33 : 458−462.
9) Nagao K, Fujii K, Saito K, et al. : Entire *PTCH1* deletion is a common event in point mutation-negative cases with nevoid basal cell carcinoma syndrome in Japan. Clin Genet (in press).
10) Gorlin RJ : Nevoid basal-cell carcinoma syndrome. Medicine (Baltimore) 1987 ; 66 : 98−113.
11) O'Malley S, Weitman D, Olding M, et al. : Multiple neoplasms following craniospinal irradiation for medulloblastoma in a patient with nevoid basal cell carcinoma syndrome : case report. J Neurosurg 1997 ; 86 : 286−288.
12) Walter AW, Pivnick EK, Bale AE, et al. : Complications of the nevoid basal cell carcinoma syndrome: a case report. J Pediatr Hematol Oncol 1997 ; 19 : 258−262.
13) Rudin CM, Hann CL, Laterra J, et al. : Treatment of medulloblastoma with hedgehog pathway inhibitor GDC-0449. N Engl J Med 2009 ; 361 : 1173−1178.
14) Evans DG, Ladusans EJ, Rimmer S, et al. : Complications of the naevoid basal cell carcinoma syndrome: results of a population based study. J Med Genet 1993 ; 30 : 460−464.
15) Shanley S, Ratcliffe J, Hockey A, et al. : Nevoid basal cell carcinoma syndrome: review of 118 affected individuals. Am J Med Genet 1994 ; 50 : 282−290.

Nevoid Basal Cell Carcinoma Syndrome: Characteristics of Clinical Manifestations and Gene Mutations in Japanese Individuals

Toshiyuki Miyashita[*1], Maiko Kiryu[*1], Kayoko Saito[*2], Katsuo Sugita[*3], Mamiko Endo[*4], Katsunori Fujii[*4]

[*1] *Department of Molecular Genetics, Kitasato University School of Medicine*
[*2] *Institute of Medical Genetics, Tokyo Women's Medical University*
[*3] *Division of Child Health, Faculty of Education, Chiba University*
[*4] *Department of Pediatrics, Chiba University Graduate School of Medicine*

Nevoid basal cell carcinoma syndrome (NBCCS), also called Gorlin syndrome, is an autosomal dominant disorder characterized by minor anomalies and predisposition toward cancer. It is caused by mutations in the *PTCH1* gene encoding a suppressor component of a receptor complex for a secreted protein, sonic hedgehog. We performed a nation-wide surveillance of NBCCS and reviewed the findings of 311 affected individuals. The major criteria were met at frequencies ranging form 36−86% and 60% of cases were expected to have novel mutations. Of note, compared with reports from Western countries, the frequency of basal cell carcinoma (BCC) was much smaller in Japanese (38%) and the mean age of onset of BCC was much younger (37.5 years). Mutational analyses demonstreted that 91% of the NBCCS families carried *PTCH1* mutations including large deletions. Clinical diagnosis of NBCCS is not always easy because

some of the NBCCS phenotypes develop with age. Therefore, early genetic testing is advisable for the early detection of tumors and for the protection of BCCs.
Key words : tumor suppressor gene, *PTCH1*, basal cell carcinoma, keratocystic odontogenic tumor, hedgehog signaling, haploinsufficiency
(J Fam Tumor 2011 ; 11 : 14−18)

ARTICLE IN PRESS

YMGME-05205; No. of pages: 6; 4C:

Molecular Genetics and Metabolism xxx (2012) xxx–xxx

Contents lists available at SciVerse ScienceDirect

Molecular Genetics and Metabolism

journal homepage: www.elsevier.com/locate/ymgme

Simple and rapid genetic testing for citrin deficiency by screening 11 prevalent mutations in *SLC25A13*

Atsuo Kikuchi [a,*], Natsuko Arai-Ichinoi [a], Osamu Sakamoto [a], Yoichi Matsubara [b], Takeyori Saheki [c,1], Keiko Kobayashi [d], Toshihro Ohura [e], Shigeo Kure [a]

[a] Department of Pediatrics, Tohoku University Graduate School of Medicine, 1-1 Seiryo-machi, Aoba-ku, Sendai, Miyagi 980-8574, Japan
[b] Department of Medical Genetics, Tohoku University School of Medicine, 1-1 Seiryo-machi, Aoba-ku, Sendai, Miyagi 980-8574, Japan
[c] Institute for Health Sciences, Tokushima Bunri University, 180 Yamashiro-cho, Tokushima 770-8514, Japan
[d] Department of Molecular Metabolism and Biochemical Genetics, Kagoshima University, Kagoshima 890-8544, Japan
[e] Division of Pediatrics, Sendai City Hospital, 3-1 Shimizukoji, Wakabayashi-ku, Sendai, Miyagi 984-8501, Japan

ARTICLE INFO

Article history:
Received 13 November 2011
Received in revised form 29 December 2011
Accepted 30 December 2011
Available online xxxx

Keywords:
Citrin deficiency
Genetic diagnosis
Rapid diagnosis
Expanded newborn screening
SLC25A13

ABSTRACT

Citrin deficiency is an autosomal recessive disorder caused by mutations in the *SLC25A13* gene and has two disease outcomes: adult-onset type II citrullinemia and neonatal intrahepatic cholestasis caused by citrin deficiency. The clinical appearance of these diseases is variable, ranging from almost no symptoms to coma, brain edema, and severe liver failure. Genetic testing for *SLC25A13* mutations is essential for the diagnosis of citrin deficiency because chemical diagnoses are prohibitively difficult. Eleven *SLC25A13* mutations account for 95% of the mutant alleles in Japanese patients with citrin deficiency. Therefore, a simple test for these mutations is desirable. We established a 1-hour, closed-tube assay for the 11 *SLC25A13* mutations using real-time PCR. Each mutation site was amplified by PCR followed by a melting-curve analysis with adjacent hybridization probes (HybProbe, Roche). The 11 prevalent mutations were detected in seven PCR reactions. Six reactions were used to detect a single mutation each, and one reaction was used to detect five mutations that are clustered in a 21-bp region in exon 17. To test the reliability, we used this method to genotype blind DNA samples from 50 patients with citrin deficiency. Our results were in complete agreement those obtained using previously established methods. Furthermore, the mutations could be detected without difficulty using dried blood samples collected on filter paper. Therefore, this assay could be used for newborn screening and for facilitating the genetic diagnosis of citrin deficiency, especially in East Asian populations.

1. Introduction

Citrin deficiency is an autosomal recessive disorder that results from mutations in the *SLC25A13* gene [1] and causes two diseases: adult-onset type II citrullinemia (CTLN2; OMIM #603471) and neonatal intrahepatic cholestasis caused by citrin deficiency (NICCD; OMIM#605814) [1–4]. The clinical appearance of these diseases is variable and ranges from almost no symptoms to coma, brain edema, and severe liver failure requiring transplantation [5–8]. In a study of patients with NICCD, only 40% of individuals were identified by newborn screenings to have abnormalities, such as hypergalactosemia, hypermethioninemia, and hyperphenylalaninemia [9]. Other patients were referred to hospitals with suspected neonatal hepatitis or biliary atresia, due to jaundice or discolored stool [9]. Hypercitrullinemia was not observed in all patients [9]. Mutation analysis of *SLC25A13* is indispensable because of the difficulties associated with the chemical diagnosis of citrin deficiency. The *SLC25A13* mutation spectrum in citrin deficiency is heterogeneous, and more than 31 mutations of *SLC25A13* have been identified to date [1,10–18]. However, there are several predominant mutations in patients from East Asia. As shown in Table 1, 6 prevalent mutations account for 91% of the mutant alleles in the Japanese population [12,19]. Five additional mutations also occur within a 21-bp cluster in exon 17 (Table 1 and Fig. 1D). The six prevalent mutations, together with the five mutations in exon 17, account for 95% of the mutant alleles in Japan [12,19].

Several different methods, such as direct sequencing, PCR restriction fragment length polymorphism (PCR-RFLP), and denaturing high performance liquid chromatography (DHPLC), are currently used for the detection of mutations in *SLC25A13* [1,10–14,19]. However, these methods are too complex for clinical use. Direct sequencing is a standard but cumbersome method. The PCR-RFLP method is

Abbreviations: CTLN2, adult-onset type II citrullinemia; FRET, fluorescence resonance energy transfer; HRM, high resolution melting; NICCD, neonatal intrahepatic cholestasis caused by citrin deficiency; Tm, melting temperature.

* Corresponding author. Fax: +81 22 717 7290.
E-mail address: akikuchi-thk@umin.ac.jp (A. Kikuchi).
[1] Present address: Institute of Resource Development and Analysis, Kumamoto University, Kumamoto 860-0811, Japan.

1096-7192/$ – see front matter © 2012 Elsevier Inc. All rights reserved.
doi:10.1016/j.ymgme.2011.12.024

specificity (i.e., binding of the probe to a perfectly matched sequence rather than to regions with sequence mismatches).

Seven primer/probe sets were designed for this study. Fig. 1 shows a schematic diagram of the strategy for mutation detection using these primer/probe sets. Tables 1 and 2 list the primer/probe sets and corresponding sequences and primer concentrations that were used to target the 11 mutations. Primer/probe sets A, B, C, D, E, and F were designed to detect mutations [I], [II], [III], [IV], [V], and [XIX], respectively. Primer/probe set G was designed to detect the five mutations clustered on exon 17: mutations [VI], [VII], [VIII], [IX], and [XXI] (Fig. 1D). All primers and probes were synthesized based on the NCBI reference SLC25A13 gene sequence (GenBank accession no. NM_014251) with the exception of mutation [XIX]:IVS16ins3kb, which was designed according to [19].

Real-time PCR and subsequent melting curve analyses were performed in a closed tube using a 20-μL mixture on a LightCycler 1.5 (Roche Diagnostics, Tokyo, Japan). The PCR mixture contained 2.0 μL of genomic DNA (10–50 ng), 0.5 μM of forward primer, 0.5 or 0.1 μM of reverse primer, 0.2 μM of each sensor and anchor probe, and 10 μL of Premix ExTaq™ (Perfect Real Time) reagent (TaKaRa Bio Inc., Otsu, Japan).

The thermal profile conditions were identical for all seven assays and consisted of an initial denaturation step (30 s at 95 °C), followed by 45 amplification cycles with the following conditions: denaturation for 5 s at 95 °C and annealing and extension for 20 s at 60 °C. The transition rate between all steps was 20 °C/s. After amplification, the samples were held at 37 °C for 1 min, followed by the melting curve acquisition at a ramp rate of 0.15 °C/s extending to 80 °C with continuous fluorescence acquisition.

Table 2
Primers, probes and target amplicon sequences, target mutation sites, and primer concentrations.

Primer/probe set	Name	Sequences of PCR products, primer locations, probe sequences, and mutation sites (5′ to 3′)	Concentration (μmol/L)
A		GGCTATACTGAAATATGAGAAatgaaaaaagggatgtttttaaattttataatgtaaattgtaataaattggtatatttgttgcttgtgtttgttttttcccctacagac	
		gtatgaccttagcagacattgaacggattgctcctctggaagagggaactctgccCTTTAACTTGGCTGAGG (181 bp)	
	Mut1-F	GGCTATACTGAAATATGAGAA	0.5
	Mut1-R	CCTCAGCCAAGTTAAAG	0.5
	Mut1-UP	ATGTAAATTGTAATAAATTGGTATATTTGTTGCTTGTGTT-FITC	
	Mut1-DW	LC Red640-GTTTTTCCCCTACAGAC**GACC**-P	
B		GAATGCAGAACCAACGAtcaactggctcttttgtgggagaactcatgtataaaaacagctttgactgttttaagaaagtgctacgctatgaaggcttctt	
		tggactgtatagaggttagtgccacatgctcaatacctgttaggtgaaataacactcaaaggtttggtttctcatcttagtgcctGACATGAATTAGCAAGACTG (205 bp)	
	Mut2-F	GAATGCAGAACCAACGA	0.5
	Mut2-R	CAGTCTTGCTAATTCATGTC	0.1
	Mut2-UP	ACCTAACAGGTATTGAGCATGTG-FITC	
	MUt2-DW	LC Red640-CACTAA**C**CTCTATACAGTCCA-P	
C		GCAGTTCAAAGCACAGTTATTtttatatagtgagaatgtgaccagactgagatggtgttgtgtctctcctgcaggtatgcctgcagcatctttagtg	
		accctgctgatgttatcaagacgagattacaggtg	
		gctgcccggg(**gagatta**caggtggctgcccggg)ctggccaaaccaCTTACAGCGGAGTGATAGAC (175 bp)	
	Mut3-F	GCAGTTCAAAGCACAGTTATT	0.5
	Mut3-R	GTCTATCACTCCGCTGTAAG	0.5
	Mut3-UP	ACCCCTGCTGATGTTATCAAGACGAGATTACAGGT-FITC	
	Mut3-DW	LC Red640-GCTGCCCGGG**GAGATTA**-P	
D		TCAATTTATTTGAGGCTGCtggaggtaccacatcccatcaagttagtttctcctattttaatggatttaattcgctccttaacaac	
		atggaactcattagaaagatctatagcactc	
		tggctggcaccaggaaagatgttgaagtGACTAAGGGTGAGTGAGAA (164 bp)	
	Mut4-F	TCAATTTATTTGAGGCTGC	0.5
	Mut4-R	TTCTCACTCACCCTTAGTC	0.5
	Mut4-UP	AATGGATTTAATT**C**GCTCCTTAACA-FITC	
	Mut4-DW	LC Red640-ATGGAACTCATTAGAAAGATCTATAGCACTC-P	
E		TGCACAAAGATGGTTCGgtcccacttgcagcagaaattcttgctggaggctgcgtaagtacctttttgaagctctcttcattgaaaagacttgtttcac	
		atatatatcactaccatggtcaacaggtgtggactaaggcttctgttTAACCACAGATCCTGCA (162 bp)	
	Mut5-F	TGCACAAAGATGGTTCG	0.5
	Mut5-R	TGCAGGATCTGTGGTTA	0.5
	Mut5-UP	GTGAAACAAGTCTTTTCAATGAAGAGAGCTTC-FITC	
	Mut5-DW	LC Red640-AAGGTACTTA**C**GCAGCCTC-P	
F	normal allele	GGAGCTGGTGGTATGGAAataatgtgttcttaactaactctttggtatcaggtaaatttttaaaatatctaattatatctgtgatttctc	
		catttttttaaagctcgtgtatttcgatcctcaccccagtttggt	
		gtaactttgctgacttacgaattgctacagcgatggttctacattgattttggaggagtgtaagtatcatgctaaatctgctgctaaatttt	
		GGCTGCTGCTAATGCTC (244 bp)	
	insertion allele	CCATCTTCCTCCTCCCTTggcagccccgccccccgatttctccatttttttaaagctcgtgtatttcgatcctcaccccagtttggt	
		gtaactttgctgacttacgaattgctacagcgatggttctacattgatttt	
		ggaggagtgtaagtatcatgctaaatctgctgctaaattttGGCTGCTGCTAATGCTC (196 bp)	
	Mut19-N-F	GGAGCTGGTGGTATGGAA	0.5
	Mut19-ins-F	CCATCTTCCTCCTCCCTT	0.5
	Mut19-R	GAGCATTAGCAGCAGCC	0.5
	Mut19-UP	ACCAAACTGGGGTGAGGATCGAAATACACGAGCTTTAAAAAAATG-FITC	
	Mut19-N-DW	LC Red640-AGAAATCACAGATATAATTAGATATTT-P	
	Mut19-ins-DW	LC Red640-AGAAATCGGGGGGCGGGG-P	
G		TCTTAACTAACTCTTTGGTATCAGGTaaatttttaaaatatctaattatatctgtgatttctccatttttttaaagctcg	
		tgtatttcgatcctcaccccagtttggtgtaactttgc**t**gac**t**t**a(a)cg**aattgctacag**cg**a	
		tggttctacattgattttggaggagtgtaagtatcatgctaaatctgctgctaaattttGGCTGCTGCTAATGCTC (217 bp)	
	Mut6-9, 21-F	TCTTAACTAACTCTTTGGTATCAGGT	0.5
	Mut6-9, 21-R	GAGCATTAGCAGCAGCC	0.5
	Mut6-9, 21-UP	TGTATTTCGATCCTCACCCCAGTTTGGTGTAACTT-FITC	
	Mut6-9, 21-DW	LC Red640-GC**G**GACTT**ACG**AATTGCTACAG**C**GA-P	

Upper case and underlined letters indicate the locations of primers and probes, respectively. Inserted DNA is shown in parenthesis. Nucleotides in boldface were used for mutation detection.
F: forward, R: reverse, UP: upstream, DW: downstream, N: normal allele, ins: insertion allele, FITC: fluorescein isothiocyanate, P: phosphate.

Please cite this article as: A. Kikuchi, et al., Simple and rapid genetic testing for citrin deficiency by screening 11 prevalent mutations in *SLC25A13*, Mol. Genet. Metab. (2012), doi:10.1016/j.ymgme.2011.12.024

17 that is not listed in Table 1. The [XXIX] mutation is located in the anchor-probe binding site and not on the reporter-probe binding site (Fig. 1D). To examine the effect of mutations on the anchor probe, we genotyped a patient with a heterozygous [XXIX] mutation using primer/probe set G (Fig. 3F). We found no change in the melting curves between the wild-type allele and the [XXIX] allele, thereby suggesting that point mutations within the anchor probe sequence have little effect on the melting curve analysis.

3.2. Validation

The genotypes determined at Tohoku University using the proposed method and those determined at Kagoshima University using a previously published method were identical for the 11 common mutations (Table S1 in supplementary material). We performed a similar test using DNA samples purified from filter-paper blood samples to determine if this method could be used for newborn screening. The genotypes determined in both laboratories were identical for all 26 DNA samples (Table S2 in supplementary material).

3.3. Frequency of eleven prevalent mutations

We found four heterozygous carriers of mutation [I], three of mutation [II], and two of mutation [V]. In addition, primer/probe set G detected one heterozygous mutation, which was confirmed as mutation [VIII] by direct sequencing. Altogether, 10 mutations were detected in 420 Japanese healthy controls.

4. Discussion

We developed a simple and rapid genetic test using real-time PCR combined with the HybProbe system for the 11 prevalent mutations in *SLC25A13*: mutations [I], [II], [III], [IV], [V], [VI], [VII], [VIII], [IX], [XIX], and [XXI]. This genetic test is a closed-tube assay in which no post-PCR handling of the samples is required. In addition, the genotyping is completed within 1 h. This test can utilize DNA samples purified from both peripheral blood and filter-paper blood. The reliability of the test was confirmed by genotyping 76 blind DNA samples from patients with citrin deficiency, including 50 peripheral blood and 26 filter-paper blood DNA samples. Because screening for the 11 targeted mutations would identify 95% of mutant alleles in the Japanese population [19], both, one, and no mutant alleles are expected to be identified in 90.4%, 9.3%, and less than 0.3% of patients, respectively. This genetic test would be useful not only in Japan but also other East Asian countries, including China, Korea, Taiwan and Vietnam, in which the same mutations are prevalent. Our test is expected to detect 76–87% of the mutant alleles in the Chinese population [12,19,25], 95–100% in the Korean population [12,19,26], 60–68% in the Taiwanese population [27,28], and 100% in the Vietnamese population [12,19]. If we were to prepare a primer/probe set for mutation [X]:g.IVS6+5G>A [12], which is prevalent in Taiwan, the estimated sensitivity would exceed 90% in the Taiwanese population [27,28].

Recently, the high resolution melting (HRM) method was reported to be suitable for the screening of mutations in the diagnosis of citrin deficiency [28]. HRM analysis is a closed-tube assay that screens for any base changes in the amplicons. The presence of SNPs anywhere on the amplicons can affect the melting curve, thereby suggesting that HRM is not suitable for screening for known mutations, but rather, is best suited to screening for unknown mutations. When we detected one heterozygous prevalent mutation, we performed HRM screening for all 17 exons of *SLC25A13*. After HRM screening, only the HRM-positive exons were subjected to direct sequencing analysis. Several mutant alleles were identified using this approach.

The frequency of homozygotes, including compound heterozygotes, presenting *SLC25A13* mutations in the population at Kagoshima (a prefecture in the southern part of Japan) has been calculated to be 1/17,000 based on the carrier rate (1/65) [19]. The prevalence of NICCD has been also reported to be 1/17,000–34,000 [29]. In this study, the carrier rate in Miyagi (a prefecture in northern Japan) was 1/42 (95% confidential interval, 1/108–1/26), thereby yielding an estimated frequency of patients with citrin deficiency of 1/7,100. Our result, together with the previous report [19], suggests that a substantial fraction of the homozygotes or compound heterozygotes of SLC25A13 mutations was asymptomatic during the neonatal period.

The early and definitive diagnosis of citrin deficiency may be beneficial for patients with citrin deficiency by encouraging specific dietary habits and avoiding iatrogenic worsening of brain edema by glycerol infusion when patients develop encephalopathy [30,31]. Because the screening of blood citrulline levels by tandem mass analysis at birth does not detect all patients with citrin deficiency, the development of a genetic test would be welcomed. In this study, we demonstrated that genomic DNA extracted from filter paper blood samples was correctly genotyped, thereby indicating the feasibility of newborn screening using this genetic test. If 100,000 babies in the northern part of Japan were screened by this method, we would detect 14 homozygotes or compound heterozygotes with *SLC25A13* mutations and 2400 heterozygous carriers. In 2400 heterozygous carriers, we would expect to observe only 1 to 2 compound heterozygotes with one target and one non-target mutation. The estimated frequency of babies with two non-target mutations is 0.04/100,000. Our genetic method would therefore allow us to screen newborn babies efficiently. If we performed this genetic test in a high-throughput real-time PCR system, such as a 384- or 1,536-well format, the cost per sample could be lowered.

In conclusion, we have established a rapid and simple detection system using the HybProbe assay for the 11 prevalent mutations in *SLC25A13*. This system could be used to screen newborns for citrin deficiency and may facilitate the genetic diagnosis of citrin deficiency, especially in East Asian populations.

Supplementary materials related to this article can be found online at doi:10.1016/j.ymgme.2011.12.024.

Acknowledgments

The authors acknowledge the contribution of Dr. Keiko Kobayashi, who passed away on December 21th, 2010. Dr. Kobayashi discovered that the *SLC25A13* gene is responsible for citrin deficiency and devoted much of her life to elucidating the mechanism of citrin deficiency. This work was supported by grants from the Ministry of Education, Culture, Sports, Science, and Technology and the Ministry of Health, Labor, and Public Welfare.

References

[1] K. Kobayashi, D.S. Sinasac, M. Iijima, A.P. Boright, L. Begum, J.R. Lee, T. Yasuda, S. Ikeda, R. Hirano, H. Terazono, M.A. Crackower, I. Kondo, L.C. Tsui, S.W. Scherer, T. Saheki, The gene mutated in adult-onset type II citrullinaemia encodes a putative mitochondrial carrier protein, Nat. Genet. 22 (1999) 159–163.
[2] T. Ohura, K. Kobayashi, Y. Tazawa, I. Nishi, D. Abukawa, O. Sakamoto, K. Iinuma, T. Saheki, Neonatal presentation of adult-onset type II citrullinemia, Hum. Genet. 108 (2001) 87–90.
[3] Y. Tazawa, K. Kobayashi, T. Ohura, D. Abukawa, F. Nishinomiya, Y. Hosoda, M. Yamashita, I. Nagata, Y. Kono, T. Yasuda, N. Yamaguchi, T. Saheki, Infantile cholestatic jaundice associated with adult-onset type II citrullinemia, J. Pediatr. 138 (2001) 735–740.
[4] T. Tomomasa, K. Kobayashi, H. Kaneko, H. Shimura, T. Fukusato, M. Tabata, Y. Inoue, S. Ohwada, M. Kasahara, Y. Morishita, M. Kimura, T. Saheki, A. Morikawa, Possible clinical and histologic manifestations of adult-onset type II citrullinemia in early infancy, J. Pediatr. 138 (2001) 741–743.
[5] T. Shigeta, M. Kasahara, T. Kimura, A. Fukuda, K. Sasaki, K. Arai, A. Nakagawa, S. Nakagawa, K. Kobayashi, S. Soneda, H. Kitagawa, Liver transplantation for an

Please cite this article as: A. Kikuchi, et al., Simple and rapid genetic testing for citrin deficiency by screening 11 prevalent mutations in *SLC25A13*, Mol. Genet. Metab. (2012), doi:10.1016/j.ymgme.2011.12.024

HMG Advance Access published December 30, 2011

Human Molecular Genetics, 2011 *1–8*
doi:10.1093/hmg/ddr585

Mutations in genes encoding the glycine cleavage system predispose to neural tube defects in mice and humans

Ayumi Narisawa[1,2], Shoko Komatsuzaki[1], Atsuo Kikuchi[3], Tetsuya Niihori[1], Yoko Aoki[1], Kazuko Fujiwara[4], Mitsuyo Tanemura[5], Akira Hata[6], Yoichi Suzuki[6], Caroline L. Relton[7], James Grinham[8], Kit-Yi Leung[8], Darren Partridge[8], Alexis Robinson[8], Victoria Stone[8], Peter Gustavsson[9], Philip Stanier[8], Andrew J. Copp[8], Nicholas D.E. Greene[8,*], Teiji Tominaga[2], Yoichi Matsubara[1] and Shigeo Kure[1,3,*]

[1]Department of Medical Genetics, [2]Department of Neurosurgery and [3]Department of Pediatrics, Tohoku University School of Medicine, Sendai, Japan, [4]Institute for Enzyme Research, University of Tokushima, Tokushima, Japan, [5]Tanemura Women's Clinic, Nagoya, Japan, [6]Department of Public Health, Chiba University School of Medicine, Chiba, Japan, [7]Human Nutrition Research Centre, Institute for Ageing and Health, Newcastle University, Newcastle upon Tyne, UK, [8]Institute of Child Health, University College London, London, UK and [9]Department of Molecular Medicine and Surgery, Karolinska Institute, Stockholm, Sweden

Received October 26, 2011; Revised November 25, 2011; Accepted December 6, 2011

Neural tube defects (NTDs), including spina bifida and anencephaly, are common birth defects of the central nervous system. The complex multigenic causation of human NTDs, together with the large number of possible candidate genes, has hampered efforts to delineate their molecular basis. Function of folate one-carbon metabolism (FOCM) has been implicated as a key determinant of susceptibility to NTDs. The glycine cleavage system (GCS) is a multi-enzyme component of mitochondrial folate metabolism, and GCS-encoding genes therefore represent candidates for involvement in NTDs. To investigate this possibility, we sequenced the coding regions of the GCS genes: *AMT*, *GCSH* and *GLDC* in NTD patients and controls. Two unique non-synonymous changes were identified in the *AMT* gene that were absent from controls. We also identified a splice acceptor site mutation and five different non-synonymous variants in *GLDC*, which were found to significantly impair enzymatic activity and represent putative causative mutations. In order to functionally test the requirement for GCS activity in neural tube closure, we generated mice that lack GCS activity, through mutation of *AMT*. Homozygous $Amt^{-/-}$ mice developed NTDs at high frequency. Although these NTDs were not preventable by supplemental folic acid, there was a partial rescue by methionine. Overall, our findings suggest that loss-of-function mutations in GCS genes predispose to NTDs in mice and humans. These data highlight the importance of adequate function of mitochondrial folate metabolism in neural tube closure.

INTRODUCTION

Neural tube defects (NTDs), such as spina bifida and anencephaly, are severe birth defects that result from failure of closure of the neural folds during embryonic development (1). Although NTDs are among the commonest birth defects in humans, the causes are still not well understood. This is most likely due to their complex, multifactorial causation

*To whom correspondence should be addressed at: Neural Development Unit, UCL Institute of Child Health, Guilford Street, London, WC1N 1EH, UK. Email: n.greene@ucl.ac.uk (N.D.E.G.); Department of Pediatrics, Tohoku University School of Medicine, 1-1 Seiryomachi, Aobaku, Sendai 980-8574, Japan. Email: kure@med.tohoku.ac.jp (S.Ku.)